

# New features in the $Z_2 \times Z_2$ 3HDM two component DM model

Jorge C. Romão\*, Rafael Boto†, Pedro N. Figueiredo‡, João P. Silva§

Instituto Superior Técnico, Departamento de Física and CFTP  
A. Rovisco Pais 1, 1049-001, Lisboa, Portugal

November 20, 2025

## Abstract

We investigate<sup>1</sup> the constraints and phenomenology of a three Higgs doublet model (3HDM) with a  $Z_2 \times Z_2$  symmetry, featuring two inert scalar doublets that give rise to a two-component dark matter (DM) scenario. We analyze the model's vacuum structure, exploring the competition between different symmetry-breaking minima, and subject it to comprehensive theoretical and current experimental constraints. Our analysis reveals previously unexplored regions of parameter space with viable dark matter candidates. Notably, we identify scenarios where both DM particles contribute comparably to the observed relic density, offering distinctive experimental signatures that could guide future searches.

## 1 Introduction

N-Higgs Doublet Models (NHDM) offer simple yet effective extensions of the Standard Model (SM) with a variety of new features. These models allow for the possibility of CP violation, provide viable candidates for Dark Matter (DM), and possess large regions of parameter space that are experimentally accessible, particularly at the Large Hadron Collider (LHC).

A common variant is the 2HDM, which introduces besides the SM a new scalar doublet with a  $Z_2$  symmetry. This symmetry leaves the SM fields unchanged and leads to the Inert Doublet Model (IDM) scenario. In this setup, the DM particle states were initially in thermal equilibrium with the primordial plasma before decoupling via the freeze-out mechanism. The relic abundance of DM, given by  $\Omega_{\text{DM}} h^2 \approx 0.12$  (Planck, 2021)[2], is determined through the thermally averaged cross-section  $\langle \sigma v \rangle$ . The viable DM mass range

---

\*jorge.romao@tecnico.ulisboa.pt

†rafael.boto@tecnico.ulisboa.pt

‡pedro.m.figueiredo@tecnico.ulisboa.pt

§jpsilva@cftp.tecnico.ulisboa.pt

<sup>1</sup>This talk presented at the conference *My Favourite Dark Matter Model* Apr 14-17, 2025, Azores, summarizes the work published in Ref.[1].

in this model typically lies between  $M_h/2 \lesssim M_{\text{DM}} \lesssim M_h$ , or alternatively,  $500 \text{ GeV} \lesssim M_{\text{DM}}$ .

In a more complex extension, the Two Inert 3HDM introduces a  $\mathbb{Z}_2 \times \mathbb{Z}_2$  symmetry, which again does not alter the SM fields but enforces additional constraints. This symmetry forbids the decay of one sector to the other, further enhancing the stability of the DM candidate and providing new avenues for study in both direct and indirect detection experiments.

We discuss in detail all possible vacua, and the conditions guaranteeing that the double inert vacuum is indeed the global minimum. We also discuss all the collider, astrophysical and cosmological constraints which we will use in our simulations. We show that it is possible to have a DM candidate mass at any value  $[\frac{1}{2}m_h, 1000 \text{ GeV}]$ , while it is possible that both candidates contribute equally to the relic density for either  $\frac{1}{2}m_h < m_{H_1} < 80 \text{ GeV}$  or  $m_{H_1} \gtrapprox 500 \text{ GeV}$ .

## 2 The Model

We consider the  $\mathbb{Z}_2 \times \mathbb{Z}_2$  3HDM. The potential is written as[3],

$$\begin{aligned} V = & m_{11}^2 \phi_1^\dagger \phi_1 + m_{22}^2 \phi_2^\dagger \phi_2 + m_{33}^2 \phi_3^\dagger \phi_3 + \lambda_1 (\phi_1^\dagger \phi_1)^2 + \lambda_2 (\phi_2^\dagger \phi_2)^2 + \lambda_3 (\phi_3^\dagger \phi_3)^2 \\ & + \lambda_4 (\phi_1^\dagger \phi_1)(\phi_2^\dagger \phi_2) + \lambda_5 (\phi_1^\dagger \phi_1)(\phi_3^\dagger \phi_3) + \lambda_6 (\phi_2^\dagger \phi_2)(\phi_3^\dagger \phi_3) + \lambda_7 (\phi_1^\dagger \phi_2)(\phi_2^\dagger \phi_1) \\ & + \lambda_8 (\phi_1^\dagger \phi_3)(\phi_3^\dagger \phi_1) + \lambda_9 (\phi_2^\dagger \phi_3)(\phi_3^\dagger \phi_2) \\ & + \left[ \lambda_{10}'' (\phi_1^\dagger \phi_2)^2 + \lambda_{11}'' (\phi_1^\dagger \phi_3)^2 + \lambda_{12}'' (\phi_2^\dagger \phi_3)^2 + \text{h.c.} \right]. \end{aligned} \quad (1)$$

## 3 Model Consistency

### 3.1 BFB

The first thing we have to check is if the potential is bounded from below(BFB). To this end, and also to look at the possible minima we use the parameterization of Ref.[4],

$$\phi_1 = \sqrt{r_1} \begin{pmatrix} \sin \alpha_1 \\ \cos \alpha_1 e^{i\beta_1} \end{pmatrix}, \quad \phi_2 = \sqrt{r_2} e^{i\gamma} \begin{pmatrix} \sin \alpha_2 \\ \cos \alpha_2 e^{i\beta_2} \end{pmatrix}, \quad \phi_3 = \sqrt{r_3} \begin{pmatrix} 0 \\ 1 \end{pmatrix}. \quad (2)$$

The necessary and sufficient conditions for the  $\mathbb{Z}_2 \times \mathbb{Z}_2$  3HDM to be bounded from below are only known along neutral directions [5],  $\alpha_1 = \alpha_2 = 0$ . Only sufficient when considering charge breaking directions[4]. We have derived[3] a general method of obtaining sufficient conditions for 3HDM's. To obtain these we start by writing the quartic part of the potential as

$$V_4 = V_N + V_{CB} + V_{\mathbb{Z}_2 \times \mathbb{Z}_2}, \quad (3)$$

where

$$\begin{aligned} V_N = & \lambda_1 (\phi_1^\dagger \phi_1)^2 + \lambda_2 (\phi_2^\dagger \phi_2)^2 + \lambda_3 (\phi_3^\dagger \phi_3)^2 + (\lambda_4 + \lambda_7) (\phi_1^\dagger \phi_1)(\phi_2^\dagger \phi_2) \\ & + (\lambda_5 + \lambda_8) (\phi_1^\dagger \phi_1)(\phi_3^\dagger \phi_3) + (\lambda_6 + \lambda_9) (\phi_2^\dagger \phi_2)(\phi_3^\dagger \phi_3), \end{aligned} \quad (4)$$

$$V_{CB} = -\lambda_7 z_{12} - \lambda_8 z_{13} - \lambda_9 z_{23}, \quad (5)$$

$$V_{\mathbb{Z}_2 \times \mathbb{Z}_2} = \left[ \lambda_{10}'' (\phi_1^\dagger \phi_2)^2 + \lambda_{11}'' (\phi_1^\dagger \phi_3)^2 + \lambda_{12}'' (\phi_2^\dagger \phi_3)^2 + \text{h.c.} \right], \quad (6)$$

where

$$0 \leq z_{ij} = (\phi_i^\dagger \phi_i)(\phi_j^\dagger \phi_j) - (\phi_i^\dagger \phi_j)(\phi_j^\dagger \phi_i) \leq r_i r_j. \quad (7)$$

Now the idea is to find a potential lower than the original one and for which it is simple to find the BFB conditions. These will be sufficient but not necessary conditions.

$$V_4 \geq V_4^{\text{lower}} = V_N + V_{CB}^{\text{lower}} + V_{\mathbb{Z}_2 \times \mathbb{Z}_2}^{\text{lower}} \equiv \frac{1}{2} \sum_{ij} r_i A_{ij} r_j, \quad (8)$$

$$V_{CB}^{\text{lower}} = r_1 r_2 \min(0, -\lambda_7) + r_1 r_3 \min(0, -\lambda_8) + r_2 r_3 \min(0, -\lambda_9), \quad (9)$$

$$V_{\mathbb{Z}_2 \times \mathbb{Z}_2}^{\text{lower}} = -2|\lambda''_{10}|r_1 r_2 - |\lambda''_{11}|r_1 r_3 - |\lambda''_{12}|r_2 r_3, \quad (10)$$

where the  $A$  matrix is,

$$A = \begin{bmatrix} \bar{\lambda}_{11} & \bar{\lambda}_{12} & \bar{\lambda}_{13} \\ \bar{\lambda}_{12} & \bar{\lambda}_{22} & \bar{\lambda}_{23} \\ \bar{\lambda}_{13} & \bar{\lambda}_{23} & \bar{\lambda}_{33} \end{bmatrix}, \quad (11)$$

and

$$\bar{\lambda}_{11} = 2\lambda_1, \quad \bar{\lambda}_{22} = 2\lambda_2, \quad \bar{\lambda}_{33} = 2\lambda_3, \quad (12)$$

$$\bar{\lambda}_{12} = \lambda_4 + \lambda_7 + \min(0, -\lambda_7) - 2|\lambda''_{10}|, \quad (13)$$

$$\bar{\lambda}_{13} = \lambda_5 + \lambda_8 + \min(0, -\lambda_8) - 2|\lambda''_{11}|, \quad (14)$$

$$\bar{\lambda}_{23} = \lambda_6 + \lambda_9 + \min(0, -\lambda_9) - 2|\lambda''_{12}|. \quad (15)$$

The potential is BFB if the matrix  $A$  is copositive. The copositivity conditions for a  $3 \times 3$  matrix can be found in Ref.[6].

## 3.2 Vacua

We are interested in a **2-Inert** minimum,  $(0, 0, v)$ . We need to identify the parameter space with the **2-Inert** configuration as the global minimum, having for all other minima,

$$V_{\text{2Inert}} < V_{\text{X}}.$$

We now list all the possible minima, either among the neutral directions or along the charge breaking ones.

### 3.2.1 Possible Vacua: The Neutral case

We start with the vacua along the neutral directions. The most general neutral vacuum configuration may be parameterized as,

$$\langle \phi_1 \rangle = \begin{bmatrix} 0 \\ v_1 e^{i\xi_1} \end{bmatrix}, \quad \langle \phi_2 \rangle = \begin{bmatrix} 0 \\ v_2 e^{i\xi_2} \end{bmatrix}, \quad \langle \phi_3 \rangle = \begin{bmatrix} 0 \\ v_3 \end{bmatrix}. \quad (16)$$

This was studied in Ref.[7]. We use their notation for the naming of the different vacua, as shown in Tab. 1.

We have confirmed their vacua but we have found a new one that we called **F0DM0'**.

Name	vevs	Symmetry	Properties
<b>EWs</b>	(0,0,0)	$\mathbb{Z}_2 \times \mathbb{Z}'_2$	EW Symmetry
<b>2-Inert</b>	(0, 0, $v_3$ )	$\mathbb{Z}_2 \times \mathbb{Z}'_2$	SM + 2 DM candidates
<b>DM1</b>	(0, $v_2$ , $v_3$ )	$\mathbb{Z}_2$	2HDM + 1 DM candidates
<b>DM2</b>	( $v_1$ , 0, $v_3$ )	$\mathbb{Z}'_2$	2HDM + 1 DM candidates
<b>F0DM1</b>	(0, $v_2$ , 0)	$\mathbb{Z}_2$	1 DM candidates + massless fermions
<b>F0DM2</b>	( $v_1$ , 0, 0)	$\mathbb{Z}'_2$	1 DM candidates + massless fermions
<b>F0DM0</b>	( $v_1$ , $v_2$ , 0)	None	No DM candidate + massless fermions
<b>N</b>	( $v_1$ , $v_2$ , $v_3$ )	None	3HDM no DM candidate
<b>sCPv</b>	( $v_1 e^{i\xi_1}$ , $v_2 e^{i\xi_2}$ , $v_3$ )	None	Spontaneous CP violation
<b>F0DM0'</b>	( $v_1$ , $iv_2$ , 0)	None	No DM candidate + massless fermions

Table 1: List of the neutral vacua.

### 3.2.2 Possible Vacua: The Charged case

Now we turn to the charge breaking vacua. We continue to follow the notation of Ref.[7]. The list of all possible charge breaking vacua are shown in Tab. 2. As before, we have identified an extra possibility; the last entry in the table. To confirm our results we have also numerically minimized the potential with `Minuit`[8] for random initial conditions to make sure all possibilities were verified.

### 3.2.3 Global minima procedure:

To find the correct global minimum we therefore follow the steps,

- Identify all possible minima.
- Apply BFB and conditions for **2-Inert** to be global minima.
- Numerically minimize the potential with `Minuit` for random initial conditions.
- Confirm none of the points ever give a lower vacuum.
- In particular we verified that the sufficient BFB were correct has we did not find any point unbounded from below.

### 3.2.4 Other Constraints

The remaining restrictions to consider include,

- The S matrix must satisfy perturbative unitarity (use the results from[9] for all the 3HDMs).
- Agreement with the S, T and U electroweak precision parameters using the formulas from[10].
- For  $h_{125}$ , we use  $\mu_{if}^h$  from ATLAS[11] .
- For the other scalars we use `HiggsTools` 1.1.3 [12] that uses the experimental cross section limits from the LEP, the Tevatron and the LHC (at 95% C.L).
- Upper limit on the Higgs total decay width is set by [13] at  $\Gamma_{tot} \leq 9.1 \text{ MeV}$  .

Name	vevs		
CB1	$\begin{pmatrix} u_1 \\ c_1 \end{pmatrix}$	$\begin{pmatrix} u_2 \\ c_2 \end{pmatrix}$	$\begin{pmatrix} 0 \\ c_3 \end{pmatrix}$
CB2	$\begin{pmatrix} u_1 \\ 0 \end{pmatrix}$	$\begin{pmatrix} u_2 \\ c_2 \end{pmatrix}$	$\begin{pmatrix} 0 \\ c_3 \end{pmatrix}$
CB3	$\begin{pmatrix} u_1 \\ c_1 \end{pmatrix}$	$\begin{pmatrix} u_2 \\ 0 \end{pmatrix}$	$\begin{pmatrix} 0 \\ c_3 \end{pmatrix}$
CB4	$\begin{pmatrix} u_1 \\ c_1 \end{pmatrix}$	$\begin{pmatrix} u_2 \\ c_2 \end{pmatrix}$	$\begin{pmatrix} 0 \\ 0 \end{pmatrix}$
CB5	$\begin{pmatrix} 0 \\ c_1 \end{pmatrix}$	$\begin{pmatrix} u_2 \\ c_2 \end{pmatrix}$	$\begin{pmatrix} 0 \\ c_3 \end{pmatrix}$
CB6	$\begin{pmatrix} u_1 \\ c_1 \end{pmatrix}$	$\begin{pmatrix} 0 \\ c_2 \end{pmatrix}$	$\begin{pmatrix} 0 \\ c_3 \end{pmatrix}$
CB7	$\begin{pmatrix} u_1 \\ 0 \end{pmatrix}$	$\begin{pmatrix} u_2 \\ 0 \end{pmatrix}$	$\begin{pmatrix} 0 \\ c_3 \end{pmatrix}$
CB8	$\begin{pmatrix} u_1 \\ 0 \end{pmatrix}$	$\begin{pmatrix} 0 \\ 0 \end{pmatrix}$	$\begin{pmatrix} 0 \\ c_3 \end{pmatrix}$
CB9	$\begin{pmatrix} 0 \\ 0 \end{pmatrix}$	$\begin{pmatrix} u_2 \\ 0 \end{pmatrix}$	$\begin{pmatrix} 0 \\ c_3 \end{pmatrix}$
FOCB	$\begin{pmatrix} u_1 \\ c_1 \end{pmatrix}$	$\begin{pmatrix} u_2 \\ -\frac{u_1^* u_2}{c_1^*} \end{pmatrix}$	$\begin{pmatrix} 0 \\ 0 \end{pmatrix}$

Table 2: List of the charge breaking vacua.

### 3.2.5 Constraints from Dark Matter

Finally we have to comply with the constraints coming from DM. These are,

- The total relic density[2] is given by the sum of the contributions from the DM candidates,
$$\Omega_T h^2 = \Omega_{H_1} h^2 + \Omega_{H_2} h^2 = 0.1200 \pm 0.0012. \quad (17)$$
- The invisible Higgs branching ratio[14],  $Br(h \rightarrow \text{invisible}) < 0.11$ .
- From direct detection - Spin-independent (SI) scattering cross section from LZ[15] with future DARWIN/XLZD and PandaX-xT. Rescale the calculated  $\sigma$  by the relative relic density.
- From indirect detection - detect gamma rays, cosmic rays or neutrinos from DM annihilation. For GeV scale, use Fermi-LAT[16]  $\gamma$ 's in dwarf galaxies, antiproton from flux AMS[17] and  $\gamma$ 's in Galactic Center from H.E.S.S.[18].

## 4 The Scan

To perform the scan it proves useful to define[7],

$$\Lambda_1 = \frac{1}{2} (\lambda_4 + \lambda_7 + 2\lambda''_{10}), \Lambda_2 = \frac{1}{2} (\lambda_6 + \lambda_9 + 2\lambda''_{12}), \Lambda_3 = \frac{1}{2} (\lambda_5 + \lambda_8 + 2\lambda''_{11}). \quad (18)$$

The parameter space has 15 parameters that we choose as follows:

$$v^2, m_{H_1}^2, m_{H_2}^2, m_{H_3}^2 = m_{SM}^2, m_{A_1}^2, m_{A_2}^2, m_{H_1^\pm}^2, m_{H_2^\pm}^2, \Lambda_1, \Lambda_2, \Lambda_3, \lambda_1, \lambda_2, \lambda_4, \lambda_7. \quad (19)$$

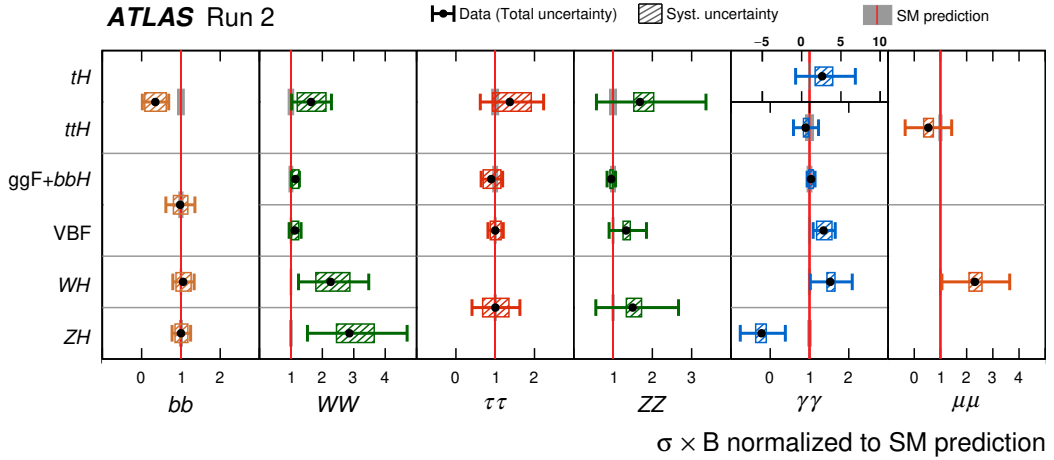


Figure 1: Signal strengths from ATLAS[11].

We choose random values in the ranges

$$\begin{aligned}
 \Lambda_1, \Lambda_2, \Lambda_3, \lambda_1, \lambda_2, \lambda_4, \lambda_7 &\in \pm [10^{-3}, 10] ; \\
 m_{H_1}, m_{H_2}, m_{A_1}, m_{A_2} &\in [50, 1000] \text{ GeV}; \\
 m_{H_1^\pm}, m_{H_2^\pm} &\in [70, 1000] \text{ GeV},
 \end{aligned} \tag{20}$$

We built a FORTRAN program for the model to calculate all the quantities for a randomly generated set of parameters and test all the constraints. We then generate the FeynRules and CalcHEP model files in order to implement the model in micrOMEGAs 6.0.5. The couplings were derived with the help of **FeynMaster**[19, 20, 21].

## 5 Results

### 5.1 Direct detection

In this section we present the results coming from applying all the constraints. First we focus in direct detection. The results are shown in Fig. 2.

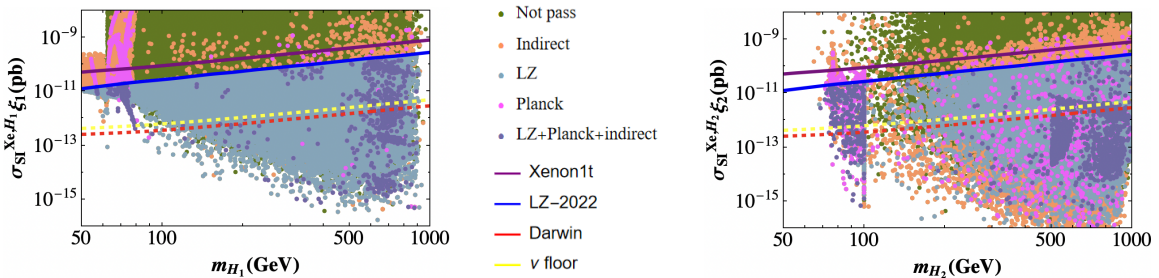


Figure 2: Direct detection constraints on  $H_1$  ( $H_2$ ) on the left (right) figure. See text for details.

The points pass all previous constraints, including collider and we take  $m_{H_2} > m_{H_1}$  always. The presence of orange/pink points above LZ line shows that this is a relevant

exclusion method. For low  $m_{H_1}$  it is possible that direct detection probes  $H_1$  without affecting  $H_2$ . We also note that final exposures of DARWIN may reach the high mass section of the neutrino floor. Then other probes must be used.

## 5.2 Indirect detection

Now we turn to the indirect constraints. Fig. 3-left shows the total  $\langle\sigma v\rangle$ . The figure

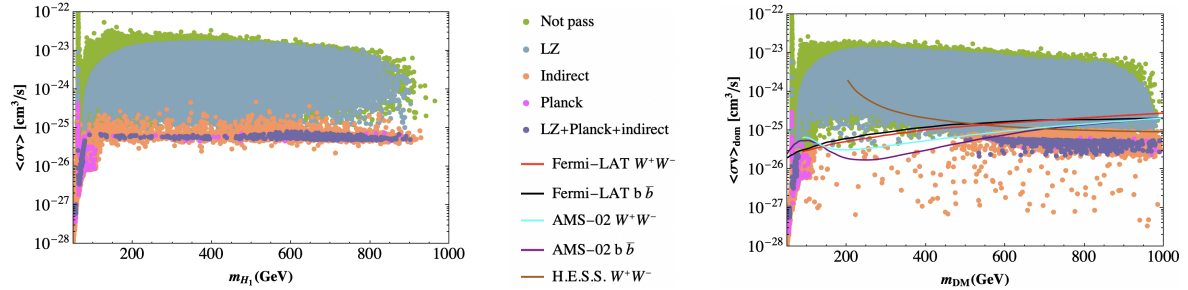


Figure 3: The colours of the points have the same meaning as in Fig. 2. The left figure shows the total  $\langle\sigma v\rangle$  as a function of  $m_{H_1}$ . The right figure shows the dominant contribution to  $\langle\sigma v\rangle$  as a function of the mass of the DM candidate,  $m_{\text{DM}}$ , which corresponds to the  $\langle\sigma v\rangle$  plotted on the vertical axis. The lines coming from Fermi-LAT [16] and H.E.S.S. [18] assume a Navarro-Frenk-White (NFW) DM density profile and the AMS-02 [17] lines correspond to the conservative approach derived in Ref. [22], with the colour codes also shown in the figure.

shows the total  $\langle\sigma v\rangle$  as a function of  $m_{H_1}$ . candidate. We assume a Navarro-Frenk-White (NFW) DM density profile. We calculate the contributing channels and take the upper limit from the reconstruction of the experimental signal for the dominant channel: above the  $W$  threshold, the annihilation proceeds mostly into  $WW$ ; it occurs into  $b\bar{b}$  otherwise. Importantly we have found that the Planck constraints (almost) guarantee indirect detection to not have effect.

## 5.3 Relic density

The results for the relic density are shown in Fig. 4. All points shown satisfy all constraints, including direct and indirect detection, and have the correct total relic density. If  $H_1$  were the only DM component, combining relic density and direct detection con-

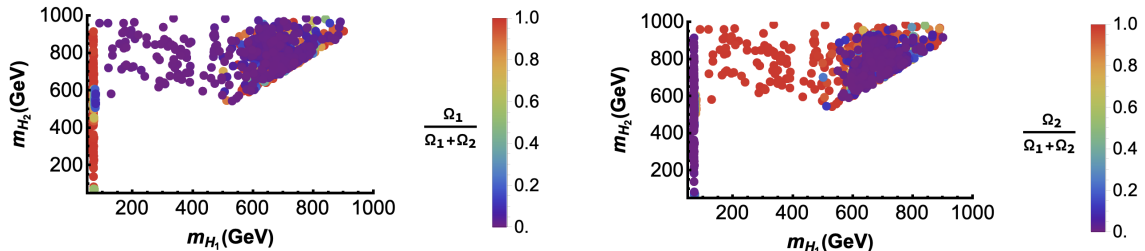


Figure 4: Range of allowed  $(m_{H_1}, m_{H_2})$  masses with a “temperature” colour code for  $\Omega_1/\Omega_T$  ( $\Omega_2/\Omega_T$ ) on the left (right).

straints would lead to the same mass regions as in the IDM. It is possible to have a

DM candidate mass at any value  $[\frac{1}{2}m_h, 1000\text{GeV}]$ . In the intermediate mass range, by requiring that it is  $H_2$  which is mostly responsible for the relic density. Equal abundance is possible for either  $\frac{1}{2}m_h < m_{H_1} < 80\text{GeV}$  or  $m_{H_1} \gtrapprox 500\text{GeV}$ .

## 6 Conclusions

In view of recent interest in multi-component DM models, we focus our attention on a  $\mathbb{Z}_2 \times \mathbb{Z}_2$  symmetric 3HDM with a double inert vacuum. We begin by revisiting the potential solutions to the stationarity equations, ensuring that our solution represents the absolute minimum. In the process, we identify two new significant minima, which we designate as F0DM0' and F0CB.

To guarantee that we account for all global minima, we must compare not only with the previously identified solutions F0DM1, F0DM2, and F0DM0, but also with these new minima: F0DM0' and F0CB.

We have derived explicit expressions for all these cases, which makes direct comparison straightforward. Additionally, we ensure consistency with key physical constraints, including unitarity, Bounded-From-Below (BFB) conditions, and compatibility with the oblique parameters  $S, T$  and  $U$ .

Following this step, we apply all current collider constraints to the parameter space of our model, including limits on the 125 GeV couplings, searches for additional scalars, and flavor observables. Next, we focus on the implications of relic density, direct detection (DD), and indirect detection (ID) of dark matter (DM).

Through an extensive scan of the parameter space, we observe that the simplistic conclusions drawn from narrow regions of the parameter space no longer hold. Instead, a much broader and more diverse range of possibilities emerges. Notably, we find regions where two distinct DM candidates contribute equally to the relic density. In the  $\mathbb{Z}_2 \times \mathbb{Z}_2$  model, the entire mass spectrum for a given component can be populated, including intermediate mass ranges where one component dominates the relic density calculation while the other plays a secondary role.

Additionally, we take into account the future sensitivity of direct detection experiments, which are expected to probe the high-mass section of the neutrino "fog" without ruling out the model. This highlights the need for complementary probes to fully test the viability of the model.

## Acknowledgments

This work is supported in part by the Portuguese FundaÃ§Ã£o para a Ciencia e Tecnologia (FCT) through the PRR (Recovery and Resilience Plan), within the scope of the investment "RE-C06-i06 - Science Plus Capacity Building", measure "RE-C06-i06.m02 - Reinforcement of financing for International Partnerships in Science, Technology and Innovation of the PRR", under the project with reference 2024.01362.CERN. The work is also supported by FCT under Contracts UIDB/00777/2020, and UIDP/00777/2020. The FCT projects are partially funded through POCTI (FEDER), COMPETE, QREN, and the EU. The work of R. Boto is also supported by FCT with the PhD grant PRT/BD/152268/2021.

## References

- [1] R. Boto, P. N. Figueiredo, J. C. Romão and J. P. Silva, *JHEP* **11**, 108 (2024), [https://doi.org/10.1007/JHEP11\(2024\)108](https://doi.org/10.1007/JHEP11(2024)108).
- [2] **Planck** Collaboration, N. Aghanim et al., *Astron. Astrophys.* **641** (2020) A6, <http://arxiv.org/abs/1807.06209> [*arXiv:1807.06209*. [Erratum: *Astron. Astrophys.* **652**, C4 (2021)].
- [3] R. Boto, J. C. Romão, and J. P. Silva, *Phys. Rev. D* **106** (2022), no. 11 115010, [\[arXiv:2208.01068\]](http://arxiv.org/abs/2208.01068).
- [4] F. S. Faro and I. P. Ivanov, *Phys. Rev. D* **100** (2019), no. 3 035038, [\[arXiv:1907.01963\]](http://arxiv.org/abs/1907.01963).
- [5] B. Grzadkowski, O. M. Ogreid, and P. Osland, *Phys. Rev. D* **80** (2009) 055013, [\[arXiv:0904.2173\]](http://arxiv.org/abs/0904.2173).
- [6] K. Kannike, *Eur. Phys. J. C* **72**, 2093 (2012) <https://doi.org/10.1140/epjc/s10052-012-2093-z>, [*arXiv:1205.37819*].
- [7] J. Hernandez-Sanchez, V. Keus, S. Moretti, D. Rojas-Ciofalo, and D. Sokolowska, <http://arxiv.org/abs/2012.11621> [*arXiv:2012.11621*].
- [8] F. James and M. Roos, *Comput. Phys. Commun.* **10** (1975) 343--367.
- [9] M. P. Bento, J. C. Romão, and J. P. Silva, *JHEP* **08** (2022) 273, [\[arXiv:2204.13130\]](http://arxiv.org/abs/2204.13130).
- [10] W. Grimus, L. Lavoura, O. M. Ogreid, and P. Osland, *Nucl. Phys. B* **801** (2008) 81--96, [\[arXiv:0802.4353\]](http://arxiv.org/abs/0802.4353).
- [11] **ATLAS** Collaboration, G. Aad et al., *Nature* **607** (2022), no. 7917 52--59, [\[arXiv:2207.00092\]](http://arxiv.org/abs/2207.00092). [Erratum: *Nature* **612**, E24 (2022)].
- [12] H. Bahl, T. Biekötter, S. Heinemeyer, C. Li, S. Paasch, G. Weiglein, and J. Wittbrodt, *Comput. Phys. Commun.* **291** (2023) 108803, [\[arXiv:2210.09332\]](http://arxiv.org/abs/2210.09332).
- [13] **CMS** Collaboration, A. M. Sirunyan et al., *Phys. Rev. D* **99** (2019), no. 11 112003, [\[arXiv:1901.00174\]](http://arxiv.org/abs/1901.00174).
- [14] G. Aad et al. [ATLAS], *Phys. Lett. B* **842**, 137963 (2023) <https://doi.org/10.1016/j.physletb.2023.137963> [*arXiv:2301.10731*].
- [15] **LZ** Collaboration, J. Aalbers et al., *Phys. Rev. Lett.* **131** (2023), no. 4 041002, [\[arXiv:2207.03764\]](http://arxiv.org/abs/2207.03764).
- [16] **Fermi-LAT** Collaboration, M. Ackermann et al., *Phys. Rev. Lett.* **115** (2015), no. 23 231301, [\[arXiv:1503.02641\]](http://arxiv.org/abs/1503.02641)

- [17] AMS Collaboration, M. Aguilar et al., *Phys. Rev. Lett.* **117** (2016), no. 9 091103, <https://doi.org/10.1103/PhysRevLett.117.091103>.
- [18] H.E.S.S. Collaboration, H. Abdalla et al., *Phys. Rev. Lett.* **129** (2022), no. 11 111101, <http://arxiv.org/abs/2207.10471> [arXiv:2207.10471].
- [19] D. Fontes and J. C. Romão, *Comput. Phys. Commun.* **256** (2020) 107311, <http://arxiv.org/abs/1909.05876> [arXiv:1909.05876].
- [20] D. Fontes and J. C. Romão, *JHEP* **06** (2021) 016, <http://arxiv.org/abs/2103.06281> [arXiv:2103.06281]. [Erratum: *JHEP* 12, 005 (2021)].
- [21] D. Fontes and J. C. Romão, <http://arxiv.org/abs/2504.01865> [arXiv:2504.01865].
- [22] A. Reinert and M. W. Winkler, *JCAP* **01** (2018) 055, <http://arxiv.org/abs/1712.00002> [arXiv:1712.00002].